

# No self-similar aggregates with sedimentation

M. Peltomäki\* and E. K. O. Hellén†

*Laboratory of Physics, Helsinki University of Technology, P. O. Box 1100, FIN-02150 HUT, Finland*

M. J. Alava‡

*Laboratory of Physics, Helsinki University of Technology, P. O. Box 1100, FIN-02150 HUT, Finland and  
SMC-INFM, Dipartimento di Fisica, Università “La Sapienza”, P.le A. Moro 2 00185 Roma, Italy*

(Dated: February 2, 2008)

Two-dimensional cluster-cluster aggregation is studied when clusters move both diffusively and sediment with a size dependent velocity. Sedimentation breaks the rotational symmetry and the ensuing clusters are not self-similar fractals: the mean cluster width perpendicular to the field direction grows faster than the height. The mean width exhibits power-law scaling with respect to the cluster size,  $\langle r_x \rangle \sim s^{l_x}$ ,  $l_x = 0.61 \pm 0.01$ , but the mean height does not. The clusters tend to become elongated in the sedimentation direction and the ratio of the single particle sedimentation velocity to single particle diffusivity controls the degree of orientation. These results are obtained using a simulation method, which becomes the more efficient the larger the moving clusters are.

PACS numbers: 05.40-a, 05.10-a, 82.20.Wt, 82.40.Ck

## I. INTRODUCTION

Aggregation of particles and particle clusters is still of great interest not only due to the number of applications it has in chemical engineering, material sciences, and atmosphere research but also due to its fundamental role as a simple model system for growth under non-equilibrium conditions [1, 2, 3]. The effects of the interplay of diffusive and ballistic motion in the case of fractal aggregates has been considered only recently [4, 5, 6, 7, 8, 9, 10, 11, 12, 13]. The relative strength of these two mechanisms will vary with cluster size. This is the case, for example, in colloidal suspensions, where both the diffusivity and the sedimentation velocity are usually expected to depend algebraically on cluster size. In this paper we study the effect of these two processes on the cluster structure.

The present understanding of colloidal aggregation under gravitation is as follows. According to experiments [6, 8] sedimenting clusters do not rotate, their anisotropy is independent of their size, and they have no preferred orientation. Based on a scaling relationship between cluster size and sedimentation velocity the sedimenting clusters are argued to be self-similar and their fractal dimension to be significantly larger than that in diffusion-limited aggregation. The restructuring of particles inside a cluster caused by hydrodynamic stresses was claimed to be the reason for sedimenting clusters being more compact. Recent simulations [9, 10] have shown that even without restructuring it is possible to produce clusters with an apparent fractal dimension that is close to the value observed in experiments, if there is a ve-

locity difference between clusters of different sizes. The cross-over to the sedimentation-dominated regime can be measured by directly observing the average size of the aggregates; however in this regime the fractal dimension still follows DLCA-like scaling [13].

In this article we study scaling properties of clusters, which are formed in cluster-cluster aggregation when both the diffusivity and the sedimentation velocity depend algebraically on cluster size. This induces a cross-over from diffusion-limited aggregation to a process where large clusters grow while settling by aggregating smaller clusters from a time-dependent size distribution,  $n_s(t)$ . We are mainly interested in generic features and hence concentrate on two dimensions, in which the effects of sedimentation on cluster structure can be studied with the most ease numerically. To compare our results to the existing ones, we also consider other structural characteristics on a qualitative level. For quantitative studies one should study more elaborate models with hydrodynamics and other delicate issues involved. The main focus here is on the self-similarity of aggregates, which is the crucial assumption made in the analysis of data in previous, similar studies. For this purpose, we consider the scaling of four radii as a function of cluster size. These are indicated in figure 1.

Our main result is that *sedimenting clusters are not self-similar fractals*. Hence, an algebraic relationship - as assumed a priori here - between cluster velocity and its mass does not necessarily imply self-similarity of the aggregates. The mean cluster width, considered in the direction perpendicular to the sedimentation velocity, grows algebraically as a function of cluster size but the mean cluster height does not follow a simple power-law, at least not in the size range considered. It is an open question as to whether the asymptotic scaling of the clusters transverse to the velocity follows the mean cluster width, or, vice versa; much larger simulations are needed to settle this issue. Also the principal radii of gyration,

---

\*Electronic address: ppv@fyslab.hut.fi

†Electronic address: ehe@fyslab.hut.fi

‡Electronic address: mja@fyslab.hut.fi

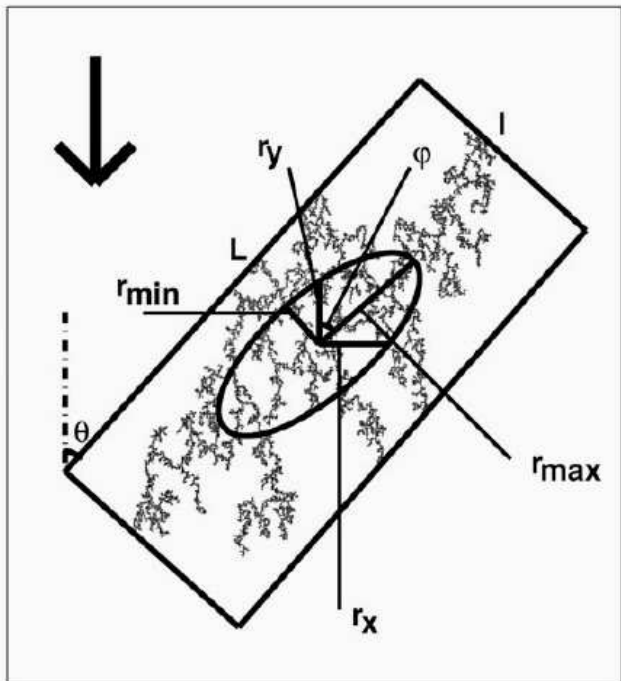


FIG. 1: Illustration of the principal radii of gyration  $r_{\min}$  and  $r_{\max}$  calculated from the radius of gyration matrix  $T$  and the radii  $r_x$  and  $r_y$ , which point perpendicular and parallel to the sedimentation velocity (shown by the thick arrow), respectively. The longer side of the rectangle shown equals to the maximal distance between any of the particles of the cluster and the angles  $\varphi$  and  $\theta$  are used to measure the orientation with respect to the direction of the sedimentation velocity.

given by the eigenvalues of the radius of gyration matrix (see Fig. 1 and Eq. (5)), grow with rates that are not equal. We present a scaling argument that explains how the width grows algebraically but simultaneously leaves the origin of the actual value of the exponent open. The fact that this particular quantity exhibits scaling brings up some interesting issues, like where does the universal, Peclet-number independent value originate from?

The difference in the growth rates indicates that clusters can not be described simply using the fractal dimension and methods relying on isotropic scaling properties. For example, studies using the radius of gyration give only an effective measure for the cluster structure. Anisotropic growth also implies that the cluster shape and its structure change in time, and we consider the former in particular in detail. We also analyze the orientation of clusters and discuss the similarities and differences between our results and previous experimental and numerical studies of the same phenomenon [8, 9, 10].

This paper is organized as follows. The model is defined in section II. A simulation method becoming the efficient the larger clusters become is introduced in section III. The scaling properties using the radius of gyration matrix are studied in section IV. Section V considers the anisotropy and orientation of clusters. Section VI

concludes the paper.

## II. MODEL

Consider fractal clusters aggregating in a suspension. The sedimentation caused by gravitation may be ignored for aggregates with characteristic radii smaller than about  $1 \mu\text{m}$ . In this region the essential features of the growth are well described by the diffusion-limited cluster-cluster aggregation (DLCA) model [1, 14]. The idea is that clusters move diffusively, and the diffusion constant depends algebraically on cluster size:  $D(s) \sim s^\gamma$ . For a cluster diffusing in a quiescent fluid it can be argued that the diffusion exponent  $\gamma = -1/d_f$ , where  $d_f$  is the fractal dimension of the cluster [15, 16, 17]. Whenever clusters (particles are clusters of size one) collide, they irreversibly aggregate together. No cluster restructuring is allowed.

Both the dynamics and the structure of clusters formed in the DLCA are well understood [1, 14]. Defining the number of clusters of size  $s$  at time  $t$  as  $n_s(t)$ , the cluster size distribution obeys dynamic scaling  $n_s(t) = S(t)^{-2} f(s/S(t))$ , where the exponent  $-2$  follows from mass conservation and the average cluster size  $S(t) = \sum_s s^2 n_s / \sum_s s n_s \sim t^z$  with  $z$  being the dynamic exponent. In two dimensions the fractal dimension of clusters is  $d_f = 1.44 \pm 0.02$  [18, 19] and including rotational diffusion or varying the value of  $\gamma$  has no essential effect on it [1, 14]. The anisotropy measured using the ratio of the principal axis of gyration is about 2.4 [20].

Here the DLCA model is considered in the presence of the sedimentation of clusters. The force exerted on a cluster sedimenting in a fluid consists of the buoyancy force  $\vec{F}_b = V \Delta \rho \vec{g}$  and the viscous drag force  $\vec{F}_d = -C \vec{v}$ , where  $V$  is the volume of the object (for an aggregate consisting of  $s$  particles it is  $s$  times the volume of a single particle),  $\Delta \rho = \rho_p - \rho_f$  is the difference between particle and fluid densities,  $\vec{g}$  is the acceleration due to gravity,  $\vec{v}$  is the sedimentation velocity and  $C$  is a positive constant depending on the specific form of the cluster [21]. For a ball of radius  $r$  the constant  $C = 6\pi\eta r$ , where  $\eta$  is the kinematic viscosity. For complicated, say fractal-like objects,  $C$  is generally unknown and we make the usual assumption that the aggregate will behave as a compact object with an effective hydrodynamic radius  $R_h$ , i.e.  $C \sim R_h$  [15, 16, 22]. If one further assumes a scaling relation between  $R_h$  and  $s$ , the sedimentation velocity depends algebraically on cluster size  $v(s) \sim s^\delta$ , where  $\delta$  is the sedimentation exponent. For a fractal one would have  $s \sim R_h^{d_f}$  resulting in  $\delta = 1 - 1/d_f$  but here we just take this as an assumption since it is not a priori clear that the ensuing clusters are fractals with respect to drag resistance. As  $\gamma < 0$  and  $\delta > 0$  aggregation is diffusion-limited for small clusters but becomes dominated by sedimentation for large ones.

The model described above neglects many issues related to real suspensions such as hydrodynamic interac-

tions, restructuring and rotation of clusters by diffusion or at aggregation to mention a few. However, our purpose is not to try to simulate all aspects of sedimentation driven aggregation but rather elucidate what kind of universal behavior one could expect to have. Hence, the results reported should be considered on a qualitative level when comparing to experiments. We discuss further these issues and the assumptions behind  $\gamma$  and  $\delta$  in the conclusions, in the light of the simulation results obtained.

A useful measure for the relative strengths of diffusion and sedimentation is the Peclet number [23]

$$P_e(s) = v(s)r/D(s), \quad (1)$$

where  $r$  is the radius of a single particle and  $v = |\vec{v}|$ . As the Peclet number depends on cluster size, in the following we use the one particle Peclet number  $Pe = P_e(1)$ . Figure 2 shows examples of clusters formed in simulations for different values of  $Pe$ .

### III. COMPUTATIONAL ASPECTS

The simulations are done on a two-dimensional lattice with periodic boundary conditions. Initially a concentration  $\phi$  of lattice sites are filled randomly. One filled lattice site is considered as a single particle. In the dynamics a particle or a cluster consisting of particles is selected randomly and time is incremented by  $N(t)^{-1}\Omega_{\max}^{-1}$ , where  $N(t)$  is the number of clusters at time  $t$  and  $\Omega_{\max}$  is the maximum mobility of any of the clusters at that time. The cluster mobility is defined as  $\Omega(s) = p_{\downarrow\downarrow}(s) + p_{\downarrow\uparrow}(s) + 2p_{\perp}(s)$ , where  $p_{\downarrow\downarrow}(s)$ ,  $p_{\downarrow\uparrow}(s)$ , and  $p_{\perp}(s)$  are proportional to the probabilities for a cluster of size  $s$  to move in the direction of the field, opposite to it and to the directions perpendicular to it, respectively. The selected cluster (of size  $s$ ) is moved if  $x < \Omega(s)/\Omega_{\max}$ , where  $x \in (0, 1)$  is a random number selected from a uniform distribution. If the selected cluster is not moved the simulation proceeds by selecting another cluster, otherwise another random number  $y \in (0, 1)$  is selected from a uniform distribution. The cluster is moved to the field direction if  $y \leq p_{\downarrow\downarrow}(s)/\Omega(s)$ , opposite to the field direction if  $p_{\downarrow\downarrow}(s)/\Omega(s) < y \leq [p_{\downarrow\downarrow}(s) + p_{\downarrow\uparrow}(s)]/\Omega(s)$ , and otherwise to one of the directions perpendicular to the field with equal probabilities ( $= p_{\perp}(s)/\Omega(s)$ ). If after the move the cluster has no overlap with others the move is accepted and another cluster is selected randomly. Otherwise the move is taken back and the cluster is aggregated with all the clusters it attempted to overlap before selecting a new cluster for the next attempt.

The terms  $p_{\downarrow\downarrow}(s)$ ,  $p_{\downarrow\uparrow}(s)$ , and  $p_{\perp}(s)$  are of the form

$$\begin{aligned} p_{\downarrow\downarrow}(s) &= (4C_{\parallel}s^{\gamma} + C_{\downarrow}s^{\delta} + C_{\downarrow}^2s^{2\delta})/2 \\ p_{\downarrow\uparrow}(s) &= (4C_{\parallel}s^{\gamma} - C_{\downarrow}s^{\delta} + C_{\downarrow}^2s^{2\delta})/2 \\ p_{\perp}(s) &= 2C_{\perp}s^{\gamma}, \end{aligned} \quad (2)$$

where  $C_{\downarrow}$ ,  $C_{\parallel}$ , and  $C_{\perp}$  are non-negative constants chosen such that  $p_{\downarrow\uparrow}(s) > 0$  for all cluster sizes. This choice gives for the sedimentation velocity  $v_s = C_{\downarrow}s^{\delta}$  and for the diffusivities  $D_{\parallel}(s) = C_{\parallel}s^{\gamma}$  and  $D_{\perp}(s) = C_{\perp}s^{\gamma}$ , in the directions parallel and perpendicular to the field, respectively. In the following we consider only the case  $C_{\parallel} = C_{\perp}$  and denote  $D(s) = D_{\parallel}(s) = D_{\perp}(s)$ . Physically, only the ratio of the sedimentation velocity to the diffusion constant is relevant and hence we report the results as a function of the one particle Peclet number  $Pe = C_{\downarrow}/C_{\perp}$ . The exponents are taken to be  $\gamma = -0.70$  and  $\delta = 0.30$ , which are obtained from relations  $\delta = 1 + \gamma$  and  $\gamma = -1/d_f$  using the fractal dimension of DLCA clusters  $d_f = 1.44$ . This is of course a valid choice initially, when DLCA is the dominating process. It should be underlined that the main point in these values is that eventually sedimentation will prevail, and that the both transfer mechanisms obey an algebraic dependence on the cluster size  $s$ .

It is known that in DLCA cluster structure, and especially the effective fractal dimension, depends on concentration [28]. In simulations reported here, the concentration is kept fixed to  $\phi = 0.01$ . The DLCA calculations are done on a lattice of size  $L_{\parallel} \times L_{\perp} = 4000 \times 4000$  and when sedimentation is included  $15000 \times 2000$  unless stated otherwise. To minimize finite size effects, all the simulations are run under the conditions that none of the particles has traveled the size of the lattice in the sedimentation direction and the size of the largest clusters is smaller than half of the lattice size in any direction.

The above choice for  $p_{\downarrow\downarrow}(s)$ ,  $p_{\downarrow\uparrow}(s)$ , and  $p_{\perp}(s)$  assumes that sedimentation does not have any effect on the diffusion properties of a cluster. This may not be the case as the velocity fluctuations of sedimenting, compact, and non-aggregating particles are larger in the sedimentation direction than perpendicular to it [24, 25, 26]. The dependence of the strength of fluctuations on aggregate size is unknown, so we make the choice of isotropic fluctuations. The precise form of fluctuations should be unimportant as the upper critical dimension for sedimentation driven aggregation is expected to be one [27].

Next we shortly discuss the implementation of the algorithm. It is constructed to be efficient for low concentrations and for large cluster sizes. Although the method is described using a two-dimensional lattice, the generalization to higher dimensions and the continuum case is straightforward.

Each cluster is represented by a virtual rectangle, whose size is the smallest possible one to enclose the cluster such that two sides of the rectangle are parallel to the sedimentation velocity (see Fig. 2). The sites belonging to a cluster are stored with respect to the, say, lower left corner of the enclosing rectangle, for two reasons. The first one is to minimize the time needed to move a cluster. Regardless of the cluster size a move can be performed by updating one single value i.e. either the  $x$ - or  $y$ -coordinate of the lower left corner of the enclosing rectangle. The second reason deals with the collisions of clusters. It is fast first to check if the rectangles overlap

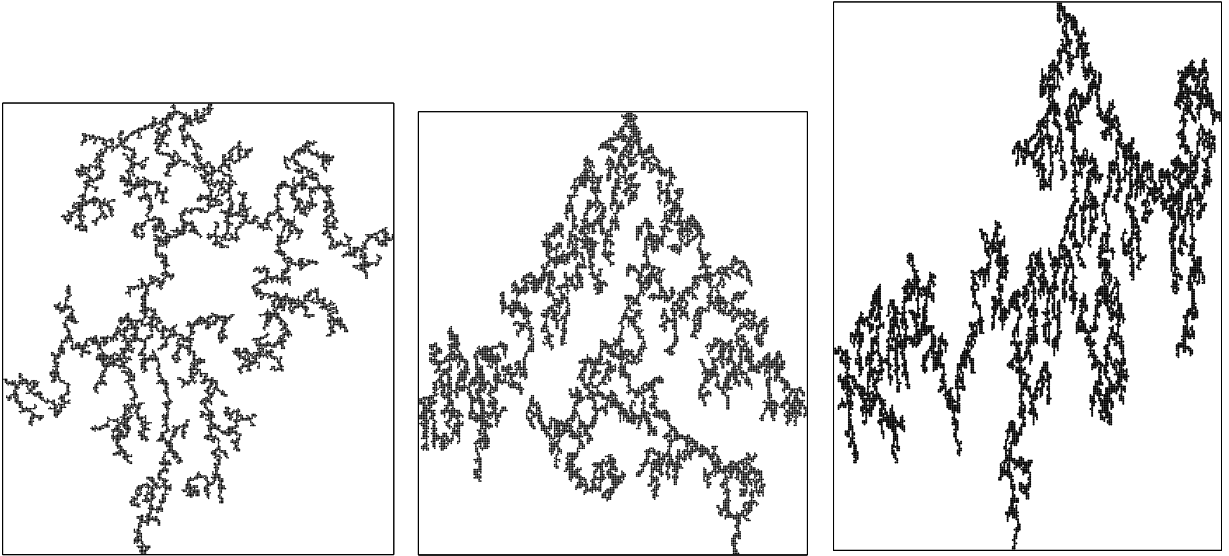


FIG. 2: Typical clusters formed in simulations for  $Pe = 0.01, 1$ , and  $10$  (from left to right). They have 41167, 87585, and 80512 particles and are contained in rectangles of size  $688 \times 942$ ,  $1169 \times 1307$  and  $1373 \times 1625$ , respectively. The sedimentation velocity points downwards.

each other and only if they do to check for the overlap of the clusters.

Obviously it would be very time-consuming to compare the rectangle that is moved to all the other rectangles. Hence, the whole system is divided into rectangular blocks and clusters are identified to belong into blocks according to the rectangles enclosing them. Then only clusters belonging to the same block(s) have to be checked.

Figure 3 compares CPU-times using the implementation described above to that with a “traditional” algorithm, where clusters are represented as occupied sites on a lattice and moved site by site. For average cluster size smaller than about ten the traditional algorithm is faster as one needs only to compare the occupancy of a few sites. On the other hand, for large clusters the method using enclosing rectangles becomes much faster, being independent of cluster size, and usually only a couple of comparisons are needed to check the overlap of a cluster with others. In the “traditional” implementation one needs of order  $S(t)$  comparisons, which slows down the computation considerably when  $S(t)$  becomes large.

In the simulations reported here the “traditional” method is used for  $S(t) < 10$  and the “rectangle” one for  $S(t) > 10$ . Hence, most of the computation time is used when the average cluster size is small. To obtain good statistics from the interesting, large cluster size region, we further apply a cloning method. It has proved to be efficient in many applications including, for example, studies of percolation clusters, native states of polymers, and reaction-diffusion systems [29]. The basic idea is simple: at a fixed average cluster size  $S_{\text{copy}}$  one makes  $n_{\text{copy}}$  copies of the cluster configuration and

continues the Monte Carlo simulation independently for each of these systems. We use  $S_{\text{copy}} = n_{\text{copy}} = 10$ . We tested that the results obtained using copying were indistinguishable from the ones obtained without it. The averages reported in this article are taken over 40 runs without copying and 10 runs which were copied 10 times. To increase the scaling window further would necessitate enormous CPU resources; even with the algorithm presented above we estimate that to augment the maximum cluster size by one order of magnitude would require of the order of one CPU-year on a fast computer.

Note that in the range of  $s$ -values shown, the typical scaling of  $S(t)$  is not algebraic manifesting a cross-over from diffusive to sedimentation-dominated dynamics [27]. Since in the asymptotic regime the mean-field dynamic exponent  $z = 1/(1 - \delta - 1/d_{\text{eff}})$ , for any reasonable value of  $d_{\text{eff}}$  (the effective fractal dimension)  $z$  will have a value much larger than unity, and the cross-over effects are noticeable since the DLCA value is much smaller.

#### IV. SCALING PROPERTIES OF CLUSTERS

Complex aggregates are often characterized by their fractal dimension  $d_f$ , which can be found by the relation of the cluster size to its characteristic radius

$$s \sim \langle R \rangle^{d_f}, \quad (3)$$

where the brackets denote averaging over clusters of size  $s$ . Usually one considers the radius of gyration

$$R_g = \sqrt{\frac{1}{s} \sum_{i=1}^s (\vec{r}_i - \vec{r}_{\text{CM}})^2}, \quad (4)$$

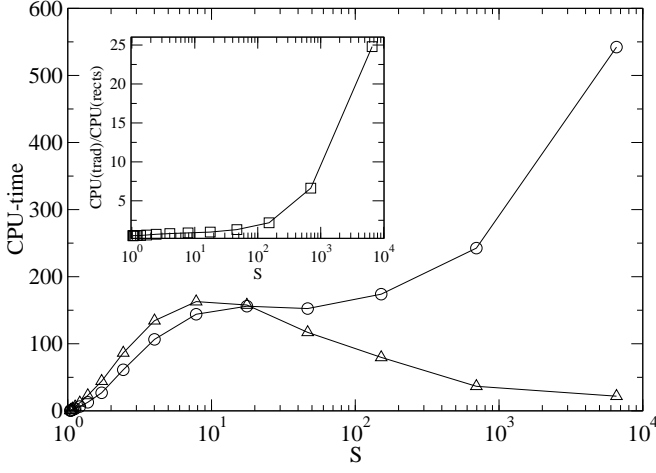


FIG. 3: CPU-time as a function of the average cluster size for 'traditional' ( $\circ$ ) and 'rectangle'-algorithms ( $\triangle$ ). Each symbol represents the time used from the previous inspection time. The inset shows the ratio of the two CPU-times.

where  $\vec{r}_i$  denotes the position of the  $i$ th particle and  $\vec{r}_{\text{CM}} = \frac{1}{s} \sum_{i=1}^s \vec{r}_i$  is the center of mass of the cluster.

As the field breaks the rotational symmetry it is not obvious that clusters will scale isotropically. Hence, we consider the radius of gyration matrix

$$T = \begin{pmatrix} T_{xx} & T_{xy} \\ T_{yx} & T_{yy} \end{pmatrix}, \quad (5)$$

where

$$T_{\alpha\beta} = \frac{1}{s} \sum_{i=1}^s (\vec{r}_{i,\alpha} - \vec{r}_{\text{CM},\alpha})(\vec{r}_{i,\beta} - \vec{r}_{\text{CM},\beta}) \quad (6)$$

and  $x$  and  $y$  refer to the  $x$ - and  $y$ -components of the position vectors. The larger and smaller eigenvalues of  $T$ , denoted by  $\lambda_{\text{max}}$  and  $\lambda_{\text{min}}$ , respectively, are related to the radius of gyration by  $R_g^2 = \lambda_{\text{max}} + \lambda_{\text{min}}$ . The square roots of the eigenvalues, called the principal radii of gyration,  $r_{\text{max,min}} = \lambda_{\text{max,min}}^{1/2}$ , may be considered as lengths of an ellipsoid describing the cluster shape and the corresponding normalized eigenvectors  $\vec{e}_{\text{max}}$  and  $\vec{e}_{\text{min}}$  define the directions of the principal axes. The preferred direction is given by the eigenvector corresponding to the larger eigenvalue. We further consider the radii in the directions perpendicular and parallel to the field, which are related to the  $T$  by the relations  $r_x = T_{xx}^{1/2}$  and  $r_y = T_{yy}^{1/2}$ , respectively, and to the radius of gyration by  $R_g^2 = r_x^2 + r_y^2$ . Figure 1 depicts the four radii for a cluster formed with  $\text{Pe} = 0.1$  and of size 90110.

Figures 4 (a) and 5 (a) show the growth of the average radii defined above as a function of the cluster size for  $\text{Pe} = 1$  and  $\text{Pe} = 10$ , respectively. Although the growth seems rather similar for different radii, the local slopes (shown in Figures 4 (b) and 5 (b)) change continuously with the cluster size. Only the radius perpendicular to

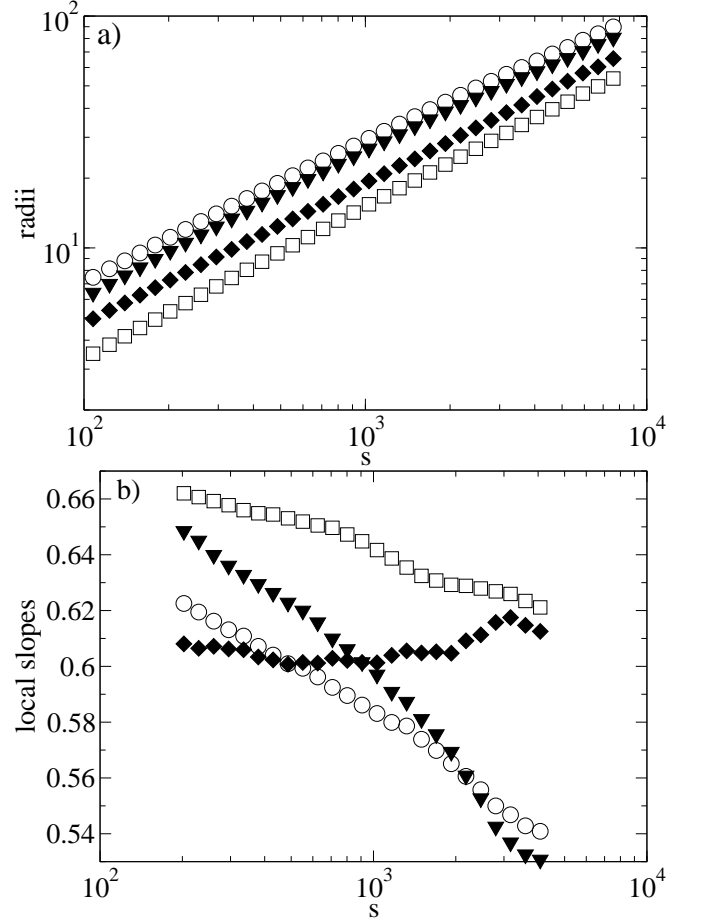


FIG. 4: (a) The mean radii  $\langle r_{\text{max}} \rangle$  ( $\circ$ ),  $\langle r_{\text{min}} \rangle$  ( $\square$ ),  $\langle r_x \rangle$  ( $\blacklozenge$ ), and  $\langle r_y \rangle$  ( $\blacktriangledown$ ) as a function of the cluster size for  $\text{Pe} = 1$ . (b) The local slopes.

the field obeys nice scaling of form  $\langle r_x \rangle \sim s^{l_x}$  with  $l_x = 0.61 \pm 0.01$ .

The overall behavior for other Peclet values ( $\text{Pe} = 0.01$  and  $0.1$ ; not shown) is rather similar and, especially, the value of  $l_x$  is independent of the Peclet number. For comparison, Figure 6 shows the scaling of the radius of gyration [Eq. (4)] as function of cluster size for various Peclet numbers. The local slopes reveal that only for the DLCA there is a scaling relation between these two. For a non-zero Peclet number one has to consider the scaling using the radius of gyration matrix [Eq. (5)] or some other observable not relying on isotropic scaling. One should emphasize that for all  $\text{Pe} > 0$  any asymptotic behavior is still far away in the range of accessible radii of gyration; the actual values reflect more the cross-over in the cluster shape and internal structure (density) than a tendency to e.g. become compact in the limit  $t \rightarrow \infty$ . This can be underlined by comparing with the scaling of the quantities, in Figs. 4 and 5.

The reasons for the existence or lack of scaling with respect to  $r_x$  and  $r_y$  can be considered by a simple scaling argument. If  $r_x$  scales with  $s$ , then also its derivative with

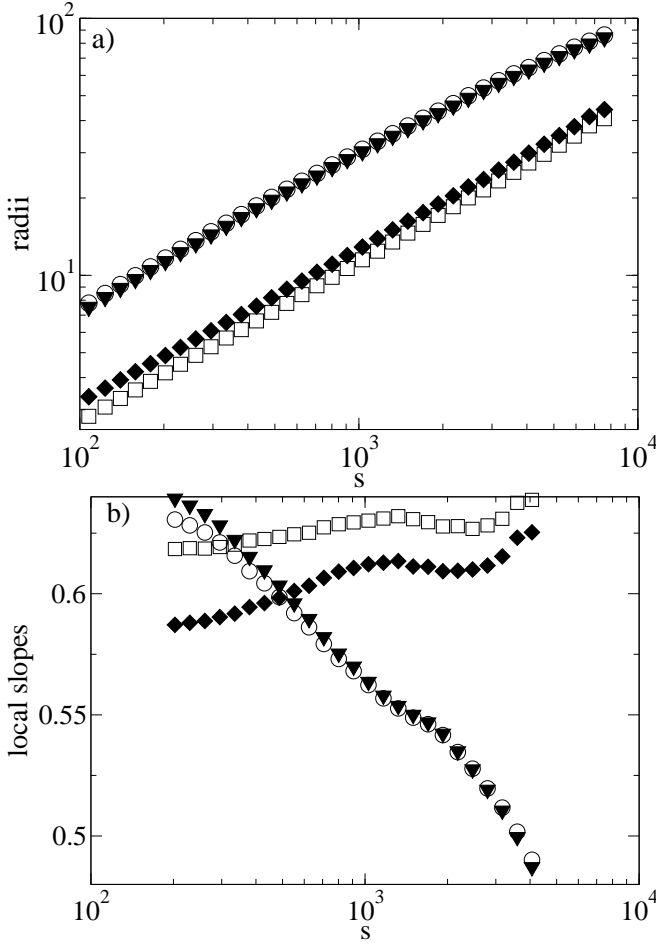


FIG. 5: (a) The mean radii  $\langle r_{\max} \rangle$  ( $\circ$ ),  $\langle r_{\min} \rangle$  ( $\square$ ),  $\langle r_x \rangle$  ( $\blacklozenge$ ), and  $\langle r_y \rangle$  ( $\blacktriangledown$ ) as a function of the cluster size for  $Pe = 10$ . (b) The local slopes.

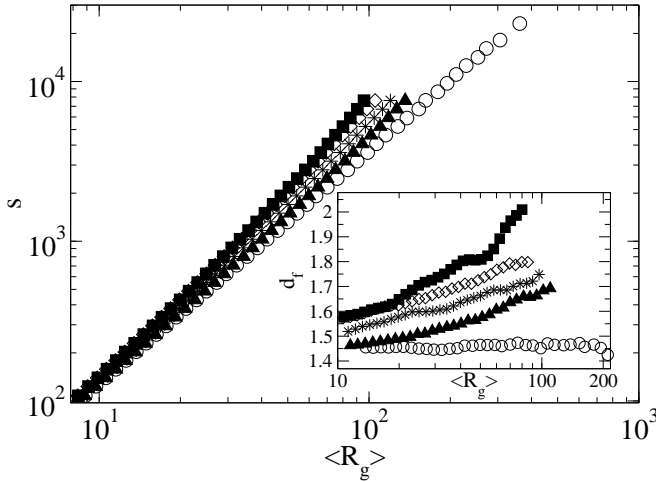


FIG. 6: Cluster size as a function of the radius of gyration for the DLCA ( $\circ$ ),  $Pe = 10$  ( $\blacksquare$ ),  $Pe = 1$  ( $\diamond$ ),  $Pe = 0.1$  ( $\star$ ), and  $Pe = 0.01$  ( $\blacktriangle$ ). The inset shows the corresponding local slopes indicating the change in the effective fractal dimension of sedimenting clusters.

respect to  $s$  does so. We have that  $\partial r_x / \partial s \approx \Delta r_x / \Delta s$  and

$$\Delta r_x = P(r_x) \times \delta r_x \quad (7)$$

where  $P(r_x)$  denotes the probability that  $r_x$  changes and  $\delta r_x$  measures the typical change in  $r_x$  per such an aggregation event.

Consider a cluster of mass  $s_1$ , which collides with another one, with  $s_2 < s_1$ . Then  $\delta r_x \sim r_x(s_2) \sim s_2^{l_x}$  and  $P(r_x) \sim r_x(s_2)/r_x(s_1) \sim (s_2/s_1)^{l_x}$ . Thus  $\partial r_x / \partial s \sim s_2^{2l_x} / (s_1^{l_x} s_2)$  and by making the ansatz  $\langle s_2 \rangle \sim a s_1$  (since  $s_2$  is cut-off by  $s_1$ ,  $a < 1$ ), we obtain that

$$\partial r_x / \partial s \sim s_1^{l_x - 1}, \quad (8)$$

exactly as one should if the growth is algebraic.

In the case of  $r_y$ , the probability  $P(r_y)$  does not have to be algebraic. This is simply so because (see Fig. 2) the roughness of the lower part of a cluster growing via sedimentation will also play a role: many of the smaller clusters will be “swallowed” inside the fjords opening downwards. It seems feasible that this leads to a change in the compactness of aggregates, which in turn results in a non-algebraic relationship between  $r_y$  and  $s$ . This is in fact a “restructuring” process, related to the changing compactness of aggregates.

Note the analogy with single cluster growth in various ballistic growth models (with shadowing, see Ch. 5.7.2 of [30]). There it is known that the bulk of the cluster becomes compact ( $d_f = d$ ), and that the boundary of the cluster undergoes interesting roughening behavior. In our case,  $l_x$  does not show signs of such a cross-over (to compact geometry) though  $l_y$  might do so asymptotically.

The equivalence to cluster growth is by no means clear in our case since the “deposited” clusters are sampled from the  $n_s(t)$  at each  $t$ , the distribution of which is broad (Fig. 7 demonstrates an example, see also ref. [31]). These clusters have a typical width-to-height ratio depending on  $s$ , making the “deposition problem” much more complicated than such ones usually are. This will remain true for any  $t$ , as the  $n_s(t)$  remains non-trivial. The implication is that for any finite Peclet number there should be a slow cross-over process that depends self-consistently on the  $n_s(t)$  and on the cluster structure that has been formed through sampling smaller clusters from the same. In any case, the fact follows that the cluster structure is anisotropic: the more recently aggregated parts of clusters are not scale-invariant with the parts that have been created earlier in the aggregation process.

Consider next the local exponents. For typical cluster sizes the local exponents of  $\langle r_{\min}(s) \rangle$  and  $\langle r_x(s) \rangle$  seem to be close to the same value (see Figs. 4 (b) and 5 (b)). Also the slopes of  $\langle r_{\max}(s) \rangle$  and  $\langle r_y(s) \rangle$  behave similarly for large cluster sizes. This indicates that the cluster are elongated in the field direction, i.e.,  $\langle r_y \rangle > \langle r_x \rangle$ . The elongation is more pronounced for high Peclet numbers.

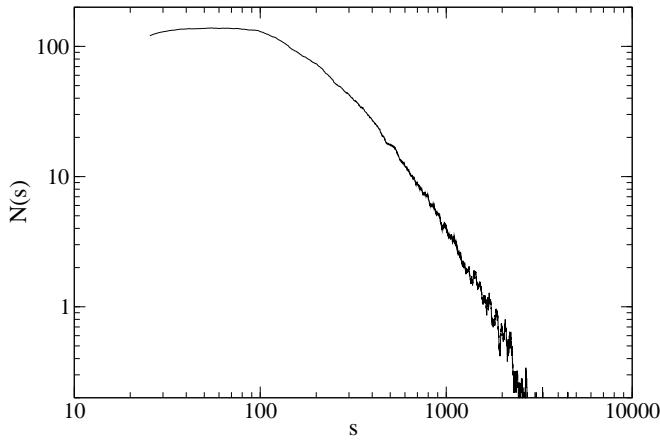


FIG. 7: The averaged (40 runs) cluster size distribution  $n_s(t)$  for  $Pe = 1$ , at  $t = 1024$ .

The same conclusion is obtained by directly considering the angular distribution using the eigenvector corresponding to the larger eigenvalue (see Section V).

Although in the size region studied  $\langle r_y \rangle > \langle r_x \rangle$ , the local slope of  $\langle r_x \rangle$  is larger than that of  $\langle r_y \rangle$  indicating that clusters grow faster in the direction perpendicular to the field. This implies that very large clusters should become elongated perpendicular to the sedimentation direction. Rough estimates for the crossover values are  $s = 8000$ ,  $80000$ , and  $300000$  for  $Pe = 0.1$ ,  $1$ , and  $10$ , respectively, and the corresponding radii of gyration  $80$ ,  $200$  and  $500$ . These values are, unfortunately, larger than we are able to simulate but should be achievable in experiments, see for example [8]. The most important conclusion, is however a choice between two asymptotic scenarios. The data implies that asymptotically  $\langle r_x(s) \rangle$  will scale with the maximum radius. Hence, should this be the case, there are two possibilities to begin with: either the maximum radius also starts to follow the  $\langle r_x(s) \rangle$ , with its scaling exponent ( $0.61$  above), or then the asymptotic scaling of both could become volume-like ( $\sim s^{0.5}$ ).

## V. ANISOTROPY AND ORIENTATION

Next we consider how the cluster shape evolves with time. To have an easily comparable measure for clusters of different sizes, we consider the scaled half-width of a cluster as a function of its scaled height  $Y = (y - y_{\min}) / (y_{\max} - y_{\min})$ , where  $y_{\max}$  and  $y_{\min}$  are the maximum and minimum  $y$ -coordinates of any of the particles in the cluster. The half-width at height  $Y$  is defined as

$$w(Y) = \frac{1}{2} \frac{x_{\max}(Y) - x_{\min}(Y)}{y_{\max} - y_{\min}}, \quad (9)$$

where  $x_{\max}$  and  $x_{\min}$  are the maximum and minimum  $x$ -coordinates of any of the particles at that height.

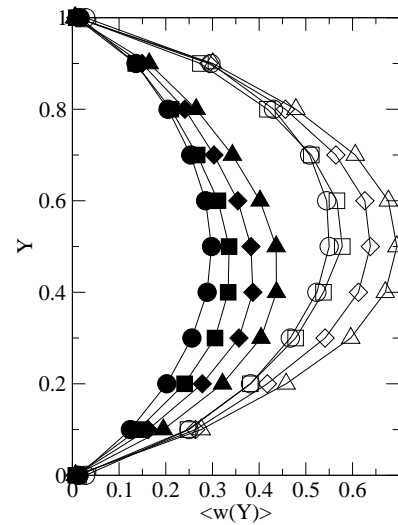


FIG. 8: Average cluster half-width as a function of scaled height for  $Pe = 0.01$  (open symbols) and  $10$  (filled symbols). The clusters are divided into four size categories:  $2500 - 5000$  ( $\circ$ ),  $5000 - 7500$  ( $\square$ ),  $7500 - 10000$  ( $\diamond$ ),  $10000 - \dots$  ( $\triangle$ ).

The relative width of a cluster increases with size as can be seen from Figure 8, in which the half-width is shown for two Peclet numbers. Note, that the relative width may well become larger than the height of a cluster. For  $Pe = 0.01$  the clusters are symmetric with respect to the point  $Y = 0.5$  but for  $Pe = 10$  they are wider at the bottom. This is due to the fact that as large clusters sediment faster than small ones they gather mass at bottom side. In other words, the upper part of a cluster is shielded by its lower part. For large clusters this results in a triangular-like shape, a particularly nice example of which is shown in Fig. 2. The sedimentation driven aggregates are sparse and have complicated scaling properties (see Figs. 4 and 5) as the clusters formed in the diffusion-dominated regime are themselves fractals. It is an open question as to what is the best characteristics of this kind of anisotropic cluster shapes. One possibility would be to look at the lower and upper parts separately (e.g. the widths thereof, after splitting the cluster at the center of mass).

The orientation of sedimenting clusters is considered using the angle  $\varphi = \arccos(\vec{e}_y \cdot \vec{e}_{\max})$  between the eigenvector corresponding to the larger eigenvalue and the unit vector in the direction of the external field. Figure 9 shows the angular distribution for two values of the Peclet number.

To study the effect of cluster size on orientation the clusters are divided in five different size classes. There is no difference in orientation with respect to cluster size. The main point, however, is that the clusters are orientated such that they prefer to have the longer principal axis aligned with the field and that the orientation distribution depends on the Peclet number. For example, for  $Pe = 10$ , there are practically no clusters with

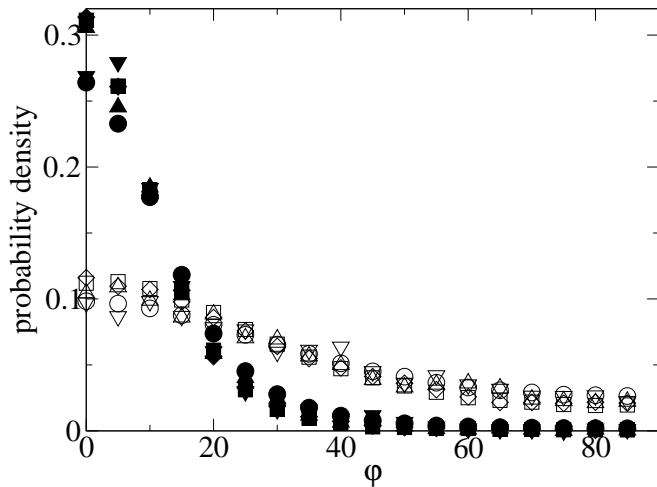


FIG. 9: Angular distribution with respect to the sedimentation direction for  $Pe = 1$  (open symbols) and  $Pe = 10$  (filled symbols) and for several size classes: 1000 – 2500 ( $\circ$ ), 2500–5000 ( $\square$ ), 5000–7500 ( $\diamond$ ), 7500 – 10000 ( $\triangle$ ) and 10000 ... ( $\nabla$ ).

$\varphi > 45^\circ$ . This is not in contrast to the conclusion made using the half-width as there is an important difference between these two approaches, when one averages them over cluster sizes. The averaging of the principal radii gives information about the typical cluster shape whereas averaging cluster width takes into account the selection of a preferred direction. We believe, that if one could simulate larger cluster sizes, another peak would start to grow at  $\varphi = 90^\circ$ .

To consider our simulations in the light of the three-dimensional experiments we also calculate cluster anisotropy and orientation as in Ref. [8]. First, a cluster is enclosed in a rectangle, whose longer sides give the maximal distance between any of the points in the cluster and the shorter ones just touch the cluster (see Fig. 1). The cluster “radius” is defined as  $R = (L + l)/4$ , where  $L$  ( $l$ ) denotes the length of the longer (shorter) edge. The orientation is measured using the angle  $\theta$  between the sedimentation velocity and the longer edge.

Figure 10 shows the average anisotropy and the average orientation angle as a function of  $R$ . The averages are taken over intervals of length one, which explains the noisiness of the data for large cluster sizes. There is a clear transient region, where both quantities vary with cluster size but for large clusters they become constant within statistical errors and the value of the anisotropy ratio  $L/l \approx 1.4$ . This is the same as the value of three-dimensional clusters [8]. However, since  $r_x$  and  $r_y$  have different scaling properties this would be a bit surprising, if it were the asymptotic value. It seems most likely that the constant value reflects more the fact that the statistics becomes sparse, with only a few clusters in this range of  $R$ . One can compare the anisotropy to the ratio of  $r_{max}$  and  $r_{min}$ ; this starts for  $s$  small from the DCLA value and is thus different. Another explanation might be

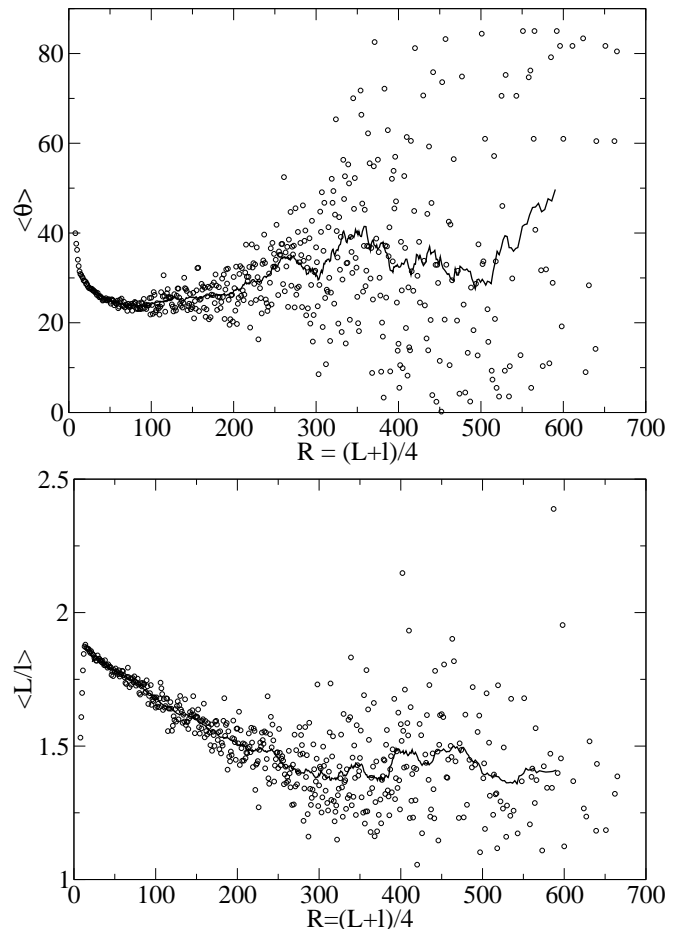


FIG. 10: a) Average orientation angle  $\langle \theta \rangle$  and b) aspect ratio  $\langle L/l \rangle$  as a function of radius  $R = (L + l)/4$  for  $Pe = 1$ . Solid lines represent sliding averages using 30 data points.

the crossover from field-elongated aggregates to ones that are wider in the direction perpendicular to the sedimentation velocity: At  $R = 300$  the cluster size  $s$  is approximately 45000, which is of the same order of magnitude than the value estimated for the crossover  $\langle r_x \rangle \approx \langle r_y \rangle$  in Sec. IV ( $s=80000$ ).

## VI. CONCLUSIONS

We have studied the structure of two-dimensional clusters, which aggregate at contact and whose motion is dominated by diffusion for small cluster sizes and by sedimentation for large ones. Considering the eigenvalues of the radius of gyration matrix, we show that due to the sedimentation the aggregates grow slower in the direction of the sedimentation velocity than perpendicular to it. Moreover, only the cluster width scales with cluster size and hence the clusters are not self-affine either, at the very least within the size range currently accessible in simulations. We underline that the data implies a cross-over scale, at which the maximal cluster radius



will begin to scale with the average cluster width, but no further conclusions can be drawn about this regime.

Interestingly, the scaling exponent characterizing the growth of the width is independent of the Peclet number, which characterizes the strength of the influence of sedimentation on aggregation. It is the one that defines “self-similarity” in the growing aggregates, but only in a limited sense since it concerns only a one-dimensional characteristics of the clusters (in contrast to e.g. a fractal dimension). The width scaling argument presented leaves open *what* the value of the width exponent would be but hints about the reasons as to why scaling is obtained in this respect, only. Here the clear conclusion is that since the Peclet number has no influence on the value ( $\approx 0.61$ ) it appears to be a universal one, and as such should be measured experimentally. The value to be obtained from three-dimensional experiments would hence be independent of the viscosity of the suspending liquid but not necessarily take the same value as obtained here. Recent experiments have shown that the radius of gyration can be used to distinguish between the DLCA and sedimentation regimes, with a clear change in the rate of increase with time [13]. However, the fractal dimension was shown to initially remain at the corresponding DLCA value. We believe this underlines the fact that in such simulations as ours it is easier to concentrate on measures that characterize the behavior of the large aggregates, as for instance  $R_g(s)$ .

Let us next discuss the justification of the simulation rules with the asymmetric growth in mind. As far as the growth is dominated by diffusion, the aggregates will be self-similar and diffusion characterized through  $D(s) \sim s^\gamma$  is reasonable. When sedimentation starts to dominate this no longer holds but then the precise characterization of diffusion is unimportant anyway. In retrospect the algebraic dependence of the sedimentation velocity on the cluster size is just a lucky choice, a posteriori justified by the fact that  $r_x$  scales algebraically. On the other hand, the relation  $\delta = 1 - 1/d_f$  is invalid. This raises the academic question that how does the value of the universal exponent  $l_x$  depend on the values of  $\gamma$  and  $\delta$ ? One may argue as follows. As the fractal dimension

of DLCA clusters is independent of  $\gamma$ , it probably does not change the scaling properties of sedimenting clusters either. However,  $\delta$  may and probably will have an effect; at least on the universality grounds there is no reason why the value of  $l_x$  would not change with  $\delta$ . It would of course be possible to attempt much more elaborate and time-consuming simulations, in which the hydrodynamic radius of each aggregate is computed self-consistently.

The anisotropic growth is also seen when studying the average form of aggregates. Larger clusters are always relatively wider than their smaller counterparts. For small Peclet numbers the clusters are rather elliptic but they became wider at the “bottom part” due to a shielding effect for large Peclet numbers. We also studied the orientation of clusters with respect to the direction of the sedimentation velocity. Clusters are oriented such that their height is larger than the width, but eventually the situation should be the opposite as the cluster width grows faster than the height. The larger the Peclet number the stronger the cluster orientation anisotropy.

The inequality of the growth rates in different direction implies that the scaling properties of sedimenting clusters can not be studied using the radius of gyration, which implicitly assumes the clusters to scale similarly in different directions. As there exist data from experiments [8] and simulations [9, 10] considering aggregation of sedimenting clusters, it would be worthwhile to check for the possibility of anisotropic growth in these cases, too. Experiments or simulations with larger aggregates could also reveal if the height of sedimenting aggregates will eventually scale with their size. It would definitely be also of interest to make simulations in the three dimensional case, and if cluster restructuring or rotational diffusion is allowed.

**Acknowledgments** - The authors thank the Academy of Finland, Center of Excellence program, for financial support. E. K. O. H. further thanks Jenny and Antti Wihuri Foundation for financial support, while M. J. A. would like to acknowledge the SMC Center, Università “La Sapienza”, Rome, for hospitality and prof. Joachim Krug for a reminder.

- 
- [1] P. Meakin, Phys. Scripta **46**, 295 (1992).
  - [2] S. K. Friedlander, *Smoke, Dust, and Haze: Fundamentals of Aerosol Dynamics*, 2nd ed. (Oxford University Press, New York, 2000).
  - [3] *Kinetics of Aggregation and Gelation*, edited by F. Family and D. P. Landau (North-Holland, Amsterdam, 1984).
  - [4] S. R. Reddy, D. H. Melik, and H. S. Fogler, J. Colloid Interface Sci. **82**, 116 (1981).
  - [5] H. Wang and R. H. Davis, J. Fluid Mech. **295**, 247 (1995).
  - [6] C. Allain, M. Cloitre, and M. Wafra, Phys. Rev. Lett. **74**, 1478 (1995).
  - [7] D. Senis and C. Allain, Phys. Rev. E **55**, 7797 (1997).
  - [8] C. Allain, M. Cloitre, and F. Parisse, J. Colloid Interface Sci. **178**, 411 (1996).
  - [9] A. E. González, Phys. Rev. Lett. **86**, 1243 (2001).
  - [10] A. E. González, J. Phys. Cond. Matter **14**, 2335 (2002).
  - [11] R. Leone *et al.*, Eur. Phys. J. E **7**, 153 (2002).
  - [12] G. Odriozola *et al.*, Phys. Rev. E **67**, 031401 (2003).
  - [13] H. Wu *et al.*, Langmuir **19**, 10710 (2003).
  - [14] P. Meakin, in *Phase Transitions and Critical Phenomena*, 1st ed., edited by C. Domb and J. L. Lebowitz (Academic Press, London, 1988), Vol. 12, Chap. 3, pp. 335–489.
  - [15] P. Wiltzius, Phys. Rev. Lett. **58**, 710 (1987).
  - [16] P. Meakin, Z.-Y. Chen, and J. M. Deutch, J. Chem. Phys. **82**, 3786 (1985).
  - [17] G. M. Wang and C. M. Sorensen, Phys. Rev. E **60**, 3036 (1999).

- [18] R. Jullien, M. Kolb, and R. Botet, J. Physique Lett. **45**, L211 (1984).
- [19] P. Meakin, Phys. Lett. **107A**, 269 (1985).
- [20] R. Botet and R. Jullien, J. Phys. A **19**, L907 (1986).
- [21] T. E. Faber, *Fluid Dynamics for Physicists*, 1st ed. (Cambridge University Press, Cambridge, 1995).
- [22] W. van Saarloos, Physica **147A**, 280 (1987).
- [23] A. J. C. Ladd, Phys. Fluids A **5**, 299 (1993).
- [24] H. Nicolai and E. Guazzelli, Phys. Fluids **7**, 3 (1995).
- [25] H. Nicolai, B. H. E. J. Hinch, L. Oger, and E. Guazzelli, Phys. Fluids **7**, 12 (1995).
- [26] W. Kalthoff, S. Schwarzer, G. H. Ristow, and H. J. Herrmann, Int. J. Mod. Phys. C **7**, 543 (1996).
- [27] E. K. O. Hellén, T. P. Simula, and M. J. Alava, Phys. Rev. E **62**, 4752 (2000).
- [28] M. Lach-hab, A. E. González, and E. Blaisten-Barojas, Phys. Rev. E **54**, 5456 (1996).
- [29] P. Grassberger, Comp. Phys. Comm. **147**, 64 (2002).
- [30] P. Meakin, *Fractals, Scaling and Growth Far From Equilibrium*. (Cambridge University Press, Cambridge, 1998).
- [31] G. Odriozola *et al.*, Physica **A335**, 35 (2004.)